

This is an Open Access document downloaded from ORCA, Cardiff University's institutional repository: <https://orca.cardiff.ac.uk/id/eprint/35178/>

This is the author's version of a work that was submitted to / accepted for publication.

Citation for final published version:

Ladak, Sam and Hicken, R. J. 2005. Evidence for hot electron magnetocurrent in a double barrier tunnel junction device. *Applied Physics Letters* 87 (23) , 232504. 10.1063/1.2140480 file

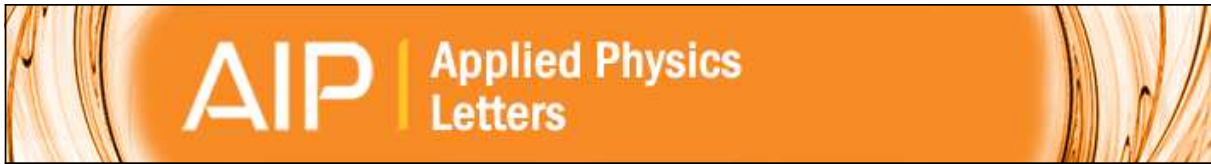
Publishers page: <http://apl.aip.org/resource/1/applab/v87/i23/p2325...>

Please note:

Changes made as a result of publishing processes such as copy-editing, formatting and page numbers may not be reflected in this version. For the definitive version of this publication, please refer to the published source. You are advised to consult the publisher's version if you wish to cite this paper.

This version is being made available in accordance with publisher policies. See <http://orca.cf.ac.uk/policies.html> for usage policies. Copyright and moral rights for publications made available in ORCA are retained by the copyright holders.





Evidence for hot electron magnetocurrent in a double barrier tunnel junction device

S. Ladak and R. J. Hicken

Citation: [Applied Physics Letters](#) **87**, 232504 (2005); doi: 10.1063/1.2140480

View online: <http://dx.doi.org/10.1063/1.2140480>

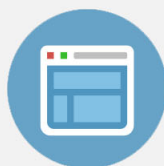
View Table of Contents: <http://scitation.aip.org/content/aip/journal/apl/87/23?ver=pdfcov>

Published by the [AIP Publishing](#)



Re-register for Table of Content Alerts

Create a profile.



Sign up today!



Evidence for hot electron magnetocurrent in a double barrier tunnel junction device

S. Ladak and R. J. Hicken^{a)}

School of Physics, University of Exeter, Stocker Road, Exeter EX4 4QL, United Kingdom

(Received 1 June 2005; accepted 13 October 2005; published online 1 December 2005)

Hot electron transport has been studied in three terminal Ta/TaO_x/Co/AlO_x/Ni₈₁Fe₁₉ structures fabricated by magnetron sputtering through shadow masks. With the Co base and Ta collector connected together via a small resistor, the collector current contains contributions first from hot electrons injected from the Ni₈₁Fe₁₉ emitter, and second from a geometrical artifact that leads to tunneling from the Fermi level in the base. Both sources of collector current lead to a room temperature magnetocurrent effect. The hot electron contribution begins to dominate as the emitter-base voltage $-V_{\text{eb}}$ exceeds 0.3 V. © 2005 American Institute of Physics.

[DOI: 10.1063/1.2140480]

Magnetic tunnel junctions (MTJ) are of great interest for use as magnetic field sensors, magnetic random access memory (MRAM) elements, and injectors and detectors within spintronic devices. Large tunnel magnetoresistance (TMR) has been obtained at low bias, where spin-polarized electrons tunnel between states close to the Fermi levels within the electrodes.^{1,2} However, while applications require large TMR at high bias, the TMR is observed to decrease rapidly with increasing bias.³ Furthermore, a semiconductor device must be placed in series with each MTJ within a MRAM array to engineer a nonlinear response suitable for matrix addressing. Recently, double barrier magnetic tunnel junctions (DBMTJ) have been considered for use in MRAM technology. The TMR exhibits a reduced bias dependence in two terminal measurements⁴ and hot electron transport may provide asymmetric I - V characteristics⁵ when a contact is made to the middle electrode.

In an earlier experimental study of hot electron transport in DBMTJs,⁶ spin-polarized hot electrons were injected from a ferromagnetic emitter (e), through an AlO_x tunnel barrier, into a ferromagnetic base (b) layer. Electrons that retained sufficient energy and momentum after spin-dependent scattering in the base were expected to enter the ferromagnetic collector (c) by crossing a second TaO_x tunnel barrier of lower height. While asymmetric plots of collector current (I_c) versus emitter-base voltage (V_{eb}) were obtained, indicating the presence of hot electron transport, I_c showed no dependence upon the applied magnetic field. The authors attributed the lack of magnetocurrent [$\text{MC} = (I_c(H_{\text{sat}}) - I_c(H))/I_c(H_{\text{sat}}) = -\Delta I_c/I_c(H_{\text{sat}})$], where H and H_{sat} are the applied field and the saturation field values, respectively, and the small TMR [$\text{TMR} = (R(H) - R(H_{\text{sat}}))/R(H_{\text{sat}})$] of the lower barrier measured at low temperature to damage caused by the etching process used to define the junctions. In a second study, a DBMTJ device was fabricated with a nonmagnetic collector.⁷ Evidence for hot electron transport was obtained by subtraction of $I_c - V_{\text{bc}}$ characteristics acquired at different values of V_{eb} , but any hot electron MC was estimated to be less than 1%. Recently, we reported the fabrication of large area Co/AlO_x/Co/AlO_x/Ni₈₁Fe₁₉ DBMTJs by magnetron sputtering through shadow masks.⁸ Both tunnel barriers

showed room temperature TMR greater than 7%, but three-terminal $I_c - V_{\text{eb}}$ measurements yielded asymmetry values $A = I_c(-V_{\text{eb}})/I_c(+V_{\text{eb}})$ of less than 1.2 for $|V_{\text{eb}}|$ values of up to 0.8 V. The collector current was also found to be orders of magnitude larger than expected for hot electron transport and was instead attributed to a geometrical artifact resulting from the finite sheet resistance of the base. Large MC values of 60% were obtained at low bias and were explained in terms of the geometrical artifact rather than a double Julliere process⁹ for which the collector current would again be much smaller. It was concluded that a lower base-collector barrier height must be used for hot electrons to dominate the MC. In this article we demonstrate a double-barrier device of structure Ta/TaO_x/Co/AlO_x/Ni₈₁Fe₁₉ that exhibits both strongly asymmetric $I_c - V_{\text{eb}}$ characteristics and a large room temperature magnetocurrent effect that we attribute to hot electron transport. DBMTJ devices of composition quartz/Ta (200 Å) / TaO_x(20 Å, 5 min)/Co (50 Å) / AlO_x (20 Å, 5 min)/Ni₈₁Fe₁₉ (200 Å) were fabricated by magnetron sputtering through shadow masks from a base pressure better than 5×10^{-7} Torr. The thickness of the deposited metal and the exposure time within the oxygen plasma have been stated for the tunnel barriers, while further details of the fabrication process may be found elsewhere.⁸ Figure 1(a) shows the deposited structure, consisting of two DBMTJs, and measurement configuration in schematic format. Both tunnel barriers were deposited through large area masks covering the majority of the substrate. Although the Ta/TaO_x bilayer is expected to contain a strong oxygen gradient, this is unimportant for the present study where the aim was to obtain a low yet resistive barrier for the efficient collection of hot electrons that have been spin filtered within the base layer. With the switch in Fig. 1(a) set to position A, the cobalt base (Co_b) and tantalum collector (Ta_c) are connected via the 100 Ω resistor R_3 . A negative bias $-V_{\text{eb}}$ is applied between the (Ni₈₁Fe₁₉)_e and Co_b electrodes so that electrons tunnel into the Co_b electrode. Electrons with sufficient energy and momentum traverse the 50 Å base layer and cross the TaO_x barrier. The collector current (I_c) causes a small voltage to develop across R_3 . For positive V_{eb} no electrons are injected into the base and no collector current is expected, leading to an asymmetric $I_c - V_{\text{eb}}$ characteristic. With the switch set to position B, negative bias is applied to the

^{a)}Electronic mail: r.j.hicken@exeter.ac.uk

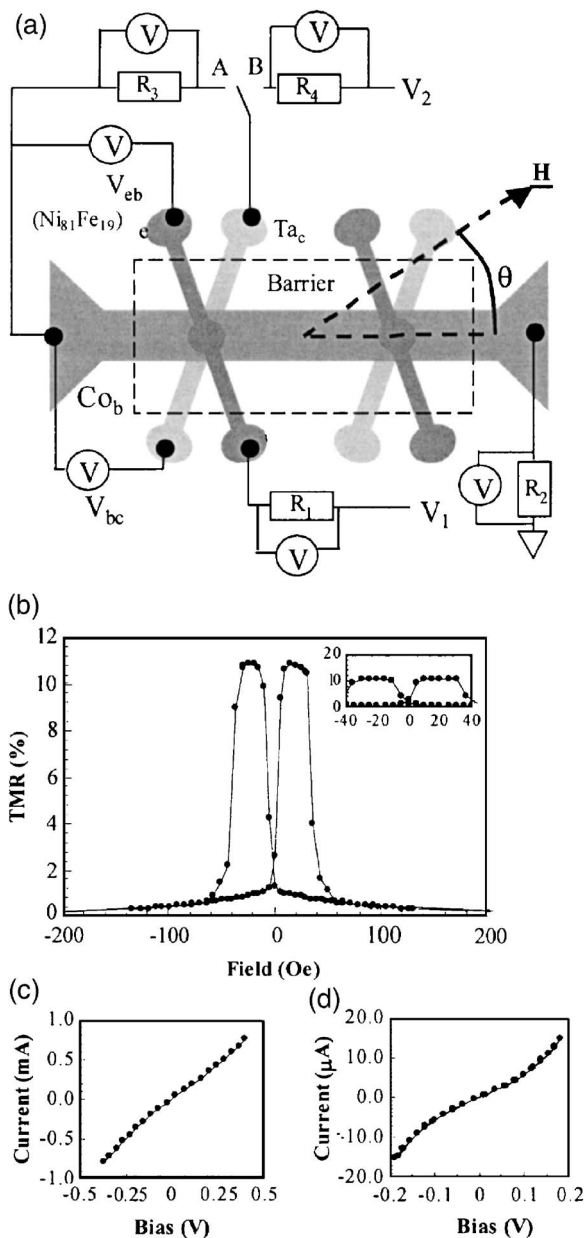


FIG. 1. (a) The DBMTJ wafer and measurement configuration are shown in schematic format. (b) The $\text{Ni}_{81}\text{Fe}_{19}$ -Co TMR. (c) The AlO_x I - V characteristic. (d) The TaO_x I - V characteristic.

$\text{Ni}_{81}\text{Fe}_{19}$ emitter to inject electrons through the AlO_x tunnel barrier, while V_{bc} is varied so as to modify the height of the TaO_x barrier and hence the hot electron transmission.

Twenty-three working DBMTJ structures were fabricated. Two terminal TMR and I - V measurements were performed to characterize the individual barriers. Resistances ranged from 460 to 1280 Ω for the $(\text{Ni}_{81}\text{Fe}_{19})_e$ - Co_b junction and from 11 to 16.8 k Ω for the Co_b - Ta_c junction. The $(\text{Ni}_{81}\text{Fe}_{19})_e$ - Co_b junction yielded TMR values between 9.4% and 11.4%, confirming the integrity of the AlO_x barrier. Since the junction resistance exceeds the electrode sheet resistance by at least one order of magnitude, current crowding is not expected to influence the emitter-base TMR. A typical TMR characteristic is shown in Fig. 1(b), while I - V characteristics for the $(\text{Ni}_{81}\text{Fe}_{19})_e$ - Co_b and Co_b - Ta_c junctions are shown in panels (c) and (d), respectively. Fits to the Simmons model¹⁰ yielded TaO_x barrier heights between 0.5 and 0.8 eV and barrier thicknesses between 26.7 and 29.3 \AA .

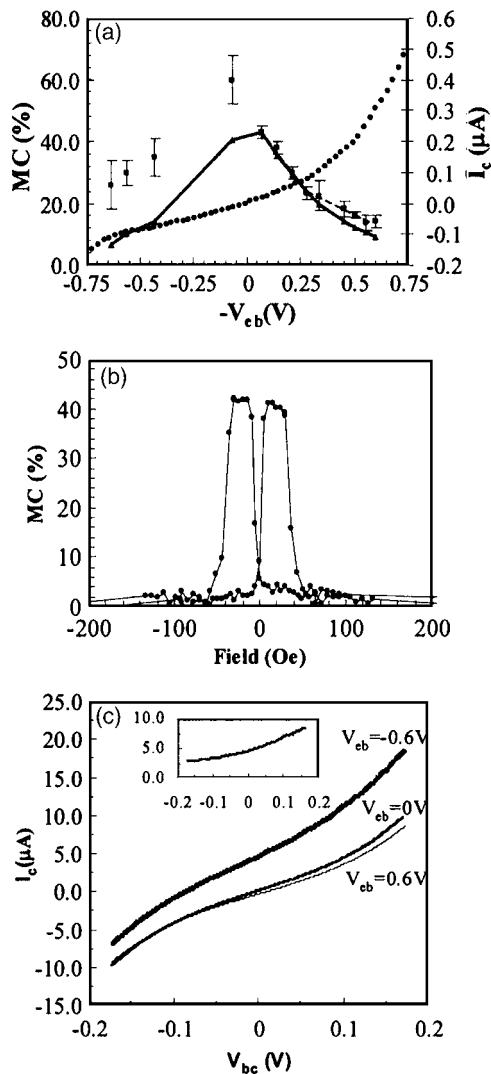


FIG. 2. (a) The I_c - V_{eb} (circles), MC - V_{eb} (squares and dashed line), and scaled TMR_{eb} - V_{eb} (triangles and solid line) characteristics. The dashed lines are guides to the eye. The TMR_{eb} has maximum value of 10.8% and has been scaled to coincide with the MC curve at $-V_{eb}=0.07$ V. (b) The MC curve for $V_{eb}=-100$ mV. (c) The I_c - V_{bc} characteristic for $V_{eb}=0$, -0.6 and $+0.6$ V, with the difference of the first two curves shown within the inset.

Strongly asymmetric ($A > 2.5$) I_c - V_{eb} characteristics were only obtained for TaO_x barrier heights less than 0.6 eV and so results will first be presented for a representative sample with a TaO_x tunnel barrier height of 0.53 eV. Figure 2(a) shows an I_c - V_{eb} characteristic (switch at position A) with an asymmetry of 3.2 at $|V_{eb}|=0.6$ V. The variation of collector MC and emitter-base TMR (TMR_{eb}) with $-V_{eb}$ is also shown in Fig. 2(a) while a typical MC curve for $V_{eb}=-0.1$ V is shown in Fig. 2(b). The shape of the latter curve is similar to that of the emitter-base TMR and was found to be independent of the applied bias. The MC is larger than the $(\text{Ni}_{81}\text{Fe}_{19})_e$ - Co_b TMR, and decreases with increasing $|V_{bc}|$. However, the rate of decrease of the MC is seen to slow at the same point, $-V_{eb}=0.3$ V, at which the asymmetry of the I_c - V_{eb} characteristic begins to noticeably increase, while the emitter-base TMR is seen to decrease more rapidly. After this first structure had failed, measurements were performed upon the other junction on the same substrate that had a fitted barrier height of 0.56 eV. With the switch in Fig. 1(a) in position B, V_{eb} was set to -0.6 , 0 , and $+0.6$ V, while V_{bc} was varied between ± 0.2 V. The resulting I_c - V_{bc} characteristics

are shown in Fig. 2(c). Strong asymmetry is observed only for $-V_{\text{eb}}=0.6$ V, whereas the curves for $-V_{\text{eb}}=0$ and $+0.6$ V are more similar in shape.

The highly asymmetric I_c-V_{eb} curve in Fig. 2(a) provides strong evidence for hot electron transport. The ideal infinite asymmetry ratio is not realized due to a nearly symmetric contribution to the collector current arising from the geometrical artifact.⁸ The finite sheet resistance of the base, $R_{b\Box}$, causes a potential difference to develop across the width of the base. This drives a current

$$I_c \approx G \frac{R_{b\Box} I_b}{R_{\text{bc}}} \quad (1)$$

through the base-collector barrier, where G is a geometry dependent factor with value of order 0.1. Since $R_{b\Box}/R_{\text{bc}} \approx 10^{-3}$ and $I_b \approx I_e$, for $V_{\text{eb}}=0.1$ V we would expect to observe a collector current in reverse bias of approximately 10^{-7} A, that is of similar magnitude to the measured value. This geometrical contribution to the collector current is also expected to be sensitive to the magnetic field. Ignoring the AMR of the base electrode, and since the base collector barrier exhibits no TMR, the change in collector current due to the applied magnetic field is given by

$$\frac{\Delta I_c}{I_c} \approx \frac{\Delta I_b}{I_b} = -(\text{TMR})_{\text{eb}}. \quad (2)$$

Comparison of Figs. 1(b) and 2(b) confirms that the collector current exhibits the same field dependence as the emitter-base TMR, however, the MC is considerably larger. We suggest that the geometrical effect can exaggerate the magnetocurrent in the same way that current crowding can enhance the TMR of single barrier MTJs.¹¹⁻¹³ In forward bias both hot electron transport and the geometrical artifact contribute to the magnetocurrent. As $-V_{\text{eb}}$ is increased additional electrons are injected into the base for which the attenuation length is expected to decrease since Fermi liquid theory predicts¹⁴ that the inelastic relaxation time varies as E^{-2} , where E is the excess energy relative to the Fermi level. However, the transmission coefficient for unscattered electrons reaching the base collector barrier has an exponential dependence upon E , and so the hot electron contribution to I_c is expected to increase rapidly with increasing bias voltage. Consequently the rapid increase in asymmetry of the I_c-V_{eb} curve that occurs when $-V_{\text{eb}}=0.3$ V marks the point at which hot electron transport begins to dominate the collector current. Since the rate of decrease of the MC slows at this same point, we infer that the hot electrons make a significant contribution to the MC. The total MC may be written as

$$\text{MC} = \left(\frac{I_{\text{Hot}}}{I_{\text{Hot}} + I_G} \right) \text{MC}_{\text{Hot}} + \left(\frac{I_G}{I_{\text{Hot}} + I_G} \right) \text{MC}_G, \quad (3)$$

where I_{Hot} and I_G , are respectively, the hot electron and geometrical artifact contributions to the collector current when the magnetic moments of the base and emitter are aligned. Since $A=3.2$ we estimate that $I_{\text{Hot}}/(I_{\text{Hot}}+I_G)=0.69$ when $-V_{\text{eb}}=0.6$ V. Assuming that $\text{MC}_G \approx 4(\text{TMR})_{\text{eb}}$ as observed in the bias range $0 < -V_{\text{eb}} < 0.3$ V where the collector current is dominated by the geometrical artifact, then we expect $\text{MC}_G \approx 9\%$ and, hence, $\text{MC}_{\text{Hot}} \approx 16\%$ when $-V_{\text{eb}}=0.6$ V. Figure 2(c) provides further evidence for hot electron transport within the DBMTJ structures. When $V_{\text{eb}}=-0.6$ V hot elec-

trons are injected into the base at an energy above the height of the TaO_x barrier. As V_{bc} is swept up and down, the base-collector barrier is effectively raised and lowered, modulating the transmission of hot electrons into the collector. The effect of electrons injected from the emitter can be isolated by subtracting the curve obtained with $V_{\text{eb}}=0$ as shown within the inset. Any difference between the curves for $V_{\text{eb}}=0$ and $+0.6$ V must be associated with the geometrical artifact although the asymmetry of the latter curve suggests that the collector current arising from the geometrical artifact and the applied base-collector bias may not superpose in a linear manner.

In summary, three-terminal transport measurements have been performed upon double barrier $\text{Ta}/\text{TaO}_x/\text{Co}/\text{AlO}_x/\text{Ni}_{81}\text{Fe}_{19}$ structures. The I_c-V_{eb} characteristics showed a maximum asymmetry of 3.2 at high bias, providing evidence for hot electron transport from the emitter to the collector. However, the collector current also contains a contribution arising from a geometrical artifact that may itself yield large MC values. Importantly the rate of decrease of MC was found to slow after $-V_{\text{eb}}$ was increased to the point at which the hot electron contribution begins to dominate, suggesting that the hot electron magnetocurrent is significant at room temperature. Further work is required to increase the hot electron MC and produce lower yet more resistive base-collector barriers that will reduce the effects of the geometrical artifact while yielding a large collector current. Further reductions might be realized immediately in lithographically defined junctions of smaller area if the integrity of the tunnel barriers can be maintained during processing. Such devices could ultimately eliminate the need for additional semiconductor devices in MRAM arrays thereby increasing the storage densities that may be achieved.

The authors gratefully acknowledge the financial support of the Engineering and Physical Sciences Research Council (EPSRC), Seagate Technology, and the New Energy and Industrial Development Organization (NEDO).

¹D. Wang, C. Nordman, J. M. Daughton, Z. Qian, and J. Fink, IEEE Trans. Magn. **40**, 2269 (2004).

²D. D. Djayapawira, K. Tsunekawa, M. Nagai, H. Maehara, S. Yamagata, N. Watanabe, S. Yuasa, Y. Suzuki, and K. Ando, Appl. Phys. Lett. **86**, 092502 (2005).

³J. S. Moodera and G. Mathon, J. Magn. Magn. Mater. **200**, 248 (1999).

⁴K. Inomata, Y. Saito, K. Nakajima, and M. Sagoi, J. Appl. Phys. **87**, 6064 (2000).

⁵M. Hehn, F. Montaigne, and A. Schuhl, Phys. Rev. B **66**, 144411 (2002).

⁶D. Lacour, M. Hehn, F. Montaigne, H. Jaffres, P. Rottlander, G. Rodary, F. Nguyen Van Dau, F. Petroff, and A. Schuhl, Europhys. Lett. **60**, 896 (2002).

⁷G. Rodary, M. Hehn, T. Dimopoulos, D. Lacour, J. Bangert, H. Jaffrès, F. Montaigne, F. Nguyen van Dau, F. Petroff, A. Schuhl, and J. Wecker, J. Magn. Magn. Mater. **290**, 1097 (2005).

⁸S. Ladak and R. J. Hicken, J. Appl. Phys. **97**, 104512 (2005).

⁹J. H. Lee, I.-W. Chang, S. J. Byun, T. K. Hong, K. Rhie, W. Y. Lee, K.-H. Shin, C. Hwang, S. S. Lee, and B. C. Lee, J. Magn. Magn. Mater. **240**, 137 (2002).

¹⁰J. G. Simmons, J. Appl. Phys. **35**, 2655 (1964).

¹¹J. S. Moodera, L. R. Kinder, J. Nowak, P. Leclair, and R. Meservey, Appl. Phys. Lett. **69**, 708 (1996).

¹²J. S. Moodera, L. R. Kinder, and J. Nowak, J. Appl. Phys. **81**, 5522 (1997).

¹³K. Matsuda, N. Watari, A. Kamijo, and H. Tsuge, Appl. Phys. Lett. **77**, 3062 (2000).

¹⁴J. J. Quinn, Phys. Rev. **126**, 1453 (1962).